Defect-Structure of Ytterbium(III) Doped Na_2SO_4 Phase I

Thomas Armbruster[1]

Laboratorium für chem. und miner. Kristallographie, Universität Bern, Freiestrasse 3, CH-3012 Bern, Switzerland

and

Reto Basler, Patric Mikhail, and Jürg Hulliger[1]

Departement für Chemie und Biochemie, Universität Bern, Freiestrasse 3, CH-3012 Bern, Switzerland

Single crystals of $Na_{1.75}Yb_{0.08}SO_4$, $Na_{1.82}Y_{0.06}SO_4$, and $Na_{1.70}Ln_{0.10}SO_4$ (Ln^{3+}=La, Yb), were grown at 1300 K by the Czochralski method. The Yb^{3+} and Y^{3+} substituted crystals transform upon cooling to a monoclinic phase intergrown in a twin relationship. However, the high-temperature defect structure of Na_2SO_4 type I can be supercooled by annealing at 1000 K and subsequent quenching. (La,Yb)-bearing crystals preserve even after moderate cooling hexagonal symmetry of Na_2SO_4 type I but display very weak and diffuse superstructure reflections indicating tripling of the c-axis. After annealing at 1000 K and subsequent quenching the superstructure reflections disappear and the (La, Yb)-substituted crystals exhibit slightly contracted cell dimensions ($a = 5.331(1)$, $c = 7.188(1)$ Å) compared to the slowly cooled crystals with the same composition ($a = 5.3472(5)$, $c = 7.2102(6)$ Å). The crystal structures of all synthesized hexagonal crystals were determined from room temperature single-crystal X-ray data and refined in space group $P6_3/mmc$. The corresponding refined structures are strongly related to the high temperature phase I of pure Na_2SO_4 but display additional SO_4 orientations correlated with the amount of substituted Y^{3+} and Ln^{3+} on Na1 and also with the number of cation vacancies on Na2 and Na3. The structures reveal a disordered arrangement of five different SO_4 orientations. If a (La,Yb)-substituted crystal is rapidly quenched from 1000 K, Ln^{3+} is concentrated together with Na at the Na1 site whereas upon slow cooling some Ln^{3+} diffuses to Na2. © 1999 Academic Press

INTRODUCTION

Yb^{3+}-based laser materials are of increasing interest. Laser action has been demonstrated for Yb-doped fluorapatites (1, 2). Yb-doped $Lu_3Al_5O_{12}$ (3) was shown to be applicable for laser diode pumping. Of similar interest are Yb-doped glasses. Mix *et al.* (4) presented an efficient CW-

laser operation of Yb-doped fluoride phosphate glass at room temperature. Hanna *et al.* (5) reported the first laser action of an Yb-doped YAG waveguide.

Yb^{3+} is an f^{13} ion, featuring only two electronic states, separated by about 10,000 cm^{-1} being hence the typical wavelength of Yb^{3+}-doped lasers. Because higher lying electronic states are missing upconversion or excited state absorption does not occur. In addition, a small quantum defect can lead to high slope efficiency (6) and low heat generation (7). The emission lifetimes of Yb^{3+}-doped materials are about a factor three to four longer than those for Nd^{3+} in the same host (8) leading to efficient pumping by laser diodes (9). These properties initiated a search for new host lattices for ytterbium in order to develop future laser materials. In this context we have investigated sodium sulfate (Na_2SO_4) as a potential laser-host crystal.

Na_2SO_4 exists in four stable crystalline modifications (phases I, II, III, and V) between room temperature and its melting point at 1156 K (10). The phase relationship and the transition temperatures are given by (11). Phase IV has been predicted (12) but lacks experimental proof (13, 14). In context of the present paper only the hexagonal high-temperature form (phase I) is of interest. This hexagonal modification with space group $P6_3/mmc$ (14) undergoes upon cooling below 503 K spontaneous displacive transformation into phase II (11). As a consequence phase I cannot be obtained at room temperature. However, phase I can be stabilized by forming solid solutions with anions such as $(CO_3)^{2-}$ or some uni-, bi-, and trivalent cations (15–17) such as K^+, Ni^{2+}, Mg^{2+}, Cu^{2+}, Co^{2+}, Y^{3+}, etc., including rare earth ions (La^{3+}, Gd^{3+}, Eu^{3+}). The general aspect of isomorphism and allotropy of A_2XO_4 and $Na_xLn(XO_4)_2$ compounds was reviewed by Bredig (18) and Vlasse *et al.* (19). Heterovalent solid solutions of Na_2SO_4 phase I accompanied by high concentrations of cation vacancies (up to 30%) give rise to a high Na^+ mobility (20).

---

[1] To whom correspondence should be addressed.

Although previous investigations are known $(11, 14, 17)$ to determine the structure of Na_2SO_4 phase I, there is still a considerable lack of knowledge on the real structure because of pronounced static and dynamic disorder. Two different sites in the Na_2SO_4 phase I are occupied by Na^+ (11, 14). If substituted by heterovalent cations one of these sites may contain vacancies whereas the other may be preferred by the guest ion (22).

In the present study we will provide a structure model how Ln^{3+} substitution modifies the host structure of Na_2SO_4 phase I. In addition, we will discuss the structural differences between a slowly cooled and a quenched crystal of $Na_{1.70}Ln_{0.10}\square_{0.20}SO_4$, $(Ln^{3+} = La, Yb)$ composition. All investigated crystals were grown by the Czochralski method to obtain sufficient crystal sizes for laser applications. The admixture of lanthanum turned out to be necessary because upon cooling crystals substituted by only Yb underwent a phase transition. As discussed below, the high temperature phase of Yb-substituted Na_2SO_4 can be supercooled by rapid quenching but in this case the quality of large single crystals suffers by the development of cracks. In addition, Y-substituted Na_2SO_4 was synthesized for comparison with literature data (17).

CRYSTAL SYNTHESIS AND CHARACTERIZATION

Starting materials for crystal synthesis were Na_2SO_4 phase V (Fluka, anhydrous, 99.9%), $Yb_2(SO_4)_3 \cdot 8\,H_2O$ and $Y_2(SO_4)_3 \cdot 8\,H_2O$ (both Aldrich, 99.9%), and $La_2(SO_4)_3 \cdot x\,H_2O$ (Aldrich, 99.9%). Powder mixture were prepared containing (a) 5 mol% $Yb_2(SO_4)_3$, (b) 3 mol% $Y_2(SO_4)_3$, (c) 4 mol% $La_2(SO_4)_3$ and 0.5 mol% $Yb_2(SO_4)_3$, and (d) 10 mol% $La_2(SO_4)_3$ (all concentrations relative to Na_2SO_4). The powder samples were heated in a porcelain crucible up to 1300 K using a resistance furnace with a heating rate of 341 K/h. Melts were kept at this temperature for 5 h in order to ensure homogeneity. Single crystals were pulled (2.5 mm/h) out of the melt by use of a rotating Pt–Rh wire (30 r/min.). Only the (La,Yb)-substituted starting material formed a colorless and transparent boule (17 mm long and 7 mm in diameter) of high optical quality. Details of crystal growth will be published elsewhere (23). Inductively coupled plasma (ICP) measurements showed that both La^{3+} and Yb^{3+} had been incorporated into the crystal when a combination of both salts was used as starting material. All other experiments led either to fragile crystals and/or to milky white colored specimens.

Single-crystal fragments (0.2–0.35 mm in dimension) were separated from boules of Y-, Yb-, (La,Yb)-, and La-substituted Na_2SO_4, glued on glass fibers, coated with epoxy resin to avoid hydration, and tested for quality on a single-crystal diffractometer. In case of the Y-, Yb-, and only La-substituted crystals the single-crystal X-ray reflections were extremely broadened and often split; thus, the forma-

tion of a monoclinic phase intergrown in a twin relationship was suspected (17). Only the (La,Yb)-substituted crystals revealed very sharp X-ray reflections. A second crystal fragment from the same (La,Yb) specimen was studied on a precession camera (Ni-filtered Cu X-radiation) where $hk0$ and hhl layers were recorded. These photographs revealed few additional weak and diffuse reflections indicating tripling of the c-axis (the strongest reflections were: 2 2 7, 1 1 11, 1 1 13, 0 0 10, 0 0 14, and their hexagonal symmetry equivalents). The latter reflections could also be located with the diffractometer but their intensities were too low and diffuse to be incorporated into a data collection.

If the samples were quenched from above 600 K, Eysel *et al.* (17) found hexagonal symmetry for Y^{3+}-substituted Na_2SO_4, corresponding to phase I. In accordance with this observation, fragments from all crystals were equilibrated at 1000 K (safely above the transition temperature at 510 K for pure Na_2SO_4) for several hours and subsequently quenched in liquid nitrogen. The crystal quality test on the single-crystal diffractometer was repeated for these quenched samples and the Yb- and Y-substituted crystals proved now to be untwinned. However, due to quenching the macroscopic quality of the crystals suffered by developing cracks. The 10% La-substituted sample still showed characteristics of intergrowth and/or twinning; thus, this composition was abandoned.

SINGLE-CRYSTAL X-RAY DATA COLLECTION AND REFINEMENT

Room temperature X-ray data were collected on an Enraf Nonius CAD4 single-crystal diffractometer using graphite monochromated Mo X-radiation. Hexagonal cell dimensions were refined from the setting angles of 25 reflections with $20° > \vartheta > 10°$ (Table 1). The few "superstructure" reflections observed for the slowly cooled (La,Yb)-substituted specimen did not allow us to establish the space group of the superstructure; thus, only an average structure of the 5×7 Å subcell was determined. Diffraction data were collected up to $\vartheta = 40°$ ($-9 \le h \le 8$, $0 \le h \le 9$, $-1 \le l \le 10$) yielding 1396 reflections of which 243 were unique. Data reduction, including background and Lorentz-polarization corrections, was performed with the program SDP (24). An empirical absorption correction using psi-scans was applied for all data sets. Systematic extinctions were in agreement with the following space group symmetries: $P6_3/mmc$, $P6_3mc$, $P\bar{3}1c$, $P31c$, $P\bar{3}2c$. Structure solutions were attempted in all five space groups using direct methods of the SHELX97 program package (25) and space group $P6_3/mmc$ was found to be correct. The structures were refined on F^2 with neutral atom scattering factors and the SHELX97 program package (25). Two S positions and three Na sites were found. The scattering power on Na1 was observed to be significantly higher than expected for only Na; thus, Na and Ln (La, Yb)

TABLE 1
Selected Structural data for Y^{3+}, Yb^{3+}, and *Ln*$^{3+}$ (La,Yb) substituted Na$_2$SO$_4$ phase I (space group *P*6$_3$/*mmc*)

Refined formula	S2-type pfu	Treatment	*a* (Å)	*c* (Å)	*R*1[a]	*nF* > 4σ(F)[b]
Na$_{1.76}$Yb$_{0.08}$□$_{0.16}$SO$_4$	0.44(3)	quenched	5.330(2)	7.187(1)	4.6	175
Na$_{1.82}$Y$_{0.06}$□$_{0.12}$SO$_4$	0.34(2)	quenched	5.347(1)	7.159(1)	4.0	148
Na$_{1.70}$*Ln*$_{0.10}$□$_{0.20}$SO$_4$	0.56(5)	quenched	5.331(1)	7.188(1)	5.0	165
Na$_{1.82}$*Ln*$_{0.06}$□$_{0.12}$SO$_4$	0.38(2)	cooled	5.3470(8)	7.2102(6)	2.9	150

[a] $R1 = (\sum \|F_o\| - F_c\|)/(\sum |F_o|)$.
[b] Number of reflections in least-squares refinement.

or Y were allowed to be varied on Na1. Due to the similar scattering behavior of La and Yb^{3+} and the low Yb^{3+} concentration in the (La,Yb)-substituted crystal these cations cannot be distinguished. Low scattering power on Na2 and Na3 indicated the presence of vacancies; thus, the Na population was allowed to vary. Low populated oxygen positions were retrieved from difference Fourier maps and vacancies on the oxygen positions O1, O2, O3 were also refined. In the final refinement cycles oxygen populations were fixed at the converged values and anisotropic displacement parameters were introduced for Na1, O1, and O2. No bond-length constraints were applied. The final least square cycles were performed with 26 parameters and 148 to 175 reflections with $F_o > 4\sigma(F_o)$ converging at $R1$ values between 2.9 and 5.0% (Table 1). Final difference Fourier maps revealed maximum residual densities of ± 0.3 electrons/Å^3.

RESULTS

In spite of the small cell dimensions and the simple chemical formula, the structure of Na$_2$SO$_4$ type I derivatives is by no means trivial (17). In addition to the arguments stated by Eysel *et al.* (17), the following observations hamper a straightforward precise refinement: (a) although the crystals were rapidly quenched from 1000 to ca. 70 K they exhibit pronounced primary and/or secondary extinction of single-crystal X-ray reflections caused by a very low degree of a mosaic defects. (b) The extreme disorder of SO$_4$ units, Na, and substituting heterovalent cations in combination with cation vacancies leads to a scaling problem. In other words, there is no position completely occupied by only one atomic species. (c) Even if diffraction data are collected up to high diffraction angles of $\vartheta = 40°$ only 242 unique reflections are obtained of which ca. 30% show no significant intensity. Data collection up to $\vartheta = 50°$ leads to 389 unique reflections but the number of unobserved intensities increases above 50%. Use of larger single crystals in order to gain higher reflection intensities is not favorable because severe secondary and/or primary extinction may also cause multiple diffraction phenomena.

The effect of severe extinction (a) was minimized by refinement of an empirical extinction parameter. The scaling problem (b) was handled by constraining the population of the two observed S sites to one S per formula unit. Furthermore, the populations of the disordered oxygen sites were constrained to obtain tetrahedral coordination for the two S sites. To reduce the number of variables and to avoid correlation problems (c) isotropic displacement parameters were used for the closely spaced Na2, Na3, S1, S2, and O3 sites.

The refined formula for quenched Na$_{1.70}$*Ln*$_{0.10}$□$_{0.20}$SO$_4$ (*Ln* = La, Yb) is in fair agreement (5.8(2)% *Ln*$^{3+}$) with the starting composition of crystal synthesis (4.5% *Ln*$^{3+}$). For the slowly cooled crystal of the same bulk composition a significantly lower concentrations of *Ln*$^{3+}$ (3.7(2)%) could be located (Table 1). The two crystals with different cooling history also show significantly different cell dimensions (Table 1). Furthermore, the slowly cooled crystal exhibits weak and diffuse superstructure reflections whereas such reflections are absent in the quenched sample. All of the above differences were confirmed by a second crystal from the same batch.

In the quenched Y- and Yb-substituted crystals 3.3(4)% Y and 4.2(2)% Yb, respectively, could be located, which is in good agreement with 3% Y and 5% Yb in the starting compositions. All refined structures are very similar and may be considered as defect varieties of Na$_2$SO$_4$ phase I. Because of this strong similarity only coordinates, populations, and displacement parameters for the slowly cooled and quenched (La,Yb)-substituted crystal are given in Tables 2a and 2b. Bond distances and selected interatomic angles (slowly cooled sample) are summarized in Table 3.

CRYSTAL STRUCTURE OF SLOWLY COOLED (La,Yb)-DOPED Na$_2$SO$_4$

Three symmetrically independent metal sites (occupied by mainly Na$^+$, minor vacancies, and *Ln*$^{3+}$) were determined. The Na1 site, at the origin (Fig. 1), exhibits a significantly higher scattering power than expected for pure Na; thus, a population of 0.938(2) Na with the reminder being *Ln*$^{3+}$ could be refined. Na2 (at 1/3, 2/3, 0.689) and Na3 (at 1/3, 2/3, 3/4) are partly occupied and only 0.45 Å apart from each other. Na2 (multiplicity 4) is 29(3)% and Na3 (multiplicity 2)

TABLE 2a
Atomic Coordinates, Populations, and Displacement Parameters ($\times 10^2$) for Slowly Cooled $Na_{1.70}Ln_{0.10}\square_{0.20}SO_4$ (Ln = La, Yb)

Atom	Pop.	x	y	z	$U_{11}{}^a$	U_{22}	U_{33}	U_{23}	U_{13}	U_{12}
S1	0.62(1)	1/3	2/3	1/4	2.58(8)					
S2	0.19(1)	1/3	2/3	0.192(1)	1.8(1)					
Na1	0.938(2)	0	0	0	3.69(7)	U_{11}	2.97(8)	0	0	$1/2U_{11}$
Ln1	0.062(2)	0	0	0	3.69(7)	U_{11}	2.97(8)	0	0	$1/2U_{11}$
Na2	0.29(3)	1/3	2/3	0.690(3)	4.2(4)					
Na3	0.27(6)	1/3	2/3	3/4	4.2(5)					
O1	0.785	0.1820(3)	2x	1/4	6.0(2)	2.0(1)	7.3(3)	0	0	$1/2U_{22}$
O2	0.212	0.239(1)	2x	0.090(2)	12.4(8)	7.4(8)	10(1)	−6.6(8)	$1/2U_{23}$	$1/2U_{22}$
O3	0.186	1/3	2/3	−0.001(4)	6.5(5)					

Note. Not all Ln^{3+} could be located.
$^a U_{11}$ or U_{iso}.

is 27(6)% occupied. Thus, Na2 and Na3 contribute with 0.85(6) Na to the formula unit. Adding 0.94 Na from Na1 yields 1.79(6) Na which agrees within one standard deviation with 1.82 Na per formula unit (pfu) required for stoichiometry.

The metal disorder is also reflected in the disordered distribution of SO_4 units. SO_4 tetrahedra alternate at 1/3, 2/3, z with disordered clusters of closely spaced Na2 and Na3 sites. There are two different S sites. S1 (multiplicity 2) at 1/3, 2/3, 1/4 is 62(1)% occupied and S2 (multiplicity 4) at 1/3, 2/3, 0.192 is 19(1)% occupied. The disorder of the various SO_4 tetrahedra is depicted in Fig. 2. There are three partially occupied O sites bonded to either S1 or S2. O1 (78% occupied) is on the mirror plane perpendicular to the threefold axis, O2 (21% occupied) is on the vertical mirror plane, and O3 (19% occupied) is on the three-fold axis. S1 bonds to two O2 and two O1, S2 bonds to three O1 and one O3. Thus O1 is common to two symmetry independent S sites. Considering the respective multiplicities, the various Na, O, and S sites contribute to the formula unit as $Na1_{0.94}La1_{0.06}Na2_{0.58}Na3_{0.27}S1_{0.62}S2_{0.38}O1_{2.35}O2_{1.27}O3_{0.38}$.

S–O distances are between 1.39 and 1.46 Å (Table 3) which is satisfactory considering the strong rotational disorder as evidenced by the strongly anisotropic displacement parameters (Fig. 2).

Na and La have very similar ionic radii in octahedral coordination 1.02 versus 1.03 Å (26). The Na1 site (Na with minor La) displays six Na1–O distances between 2.47 and 2.30 Å depending on whether O1 or O2 is locally occupied. An additional six O3 sites (low populated) occur 3.09 Å from Na1. The coordination of Na2 is difficult to define. There are either six O1 sites 2.71 Å apart or twelve O2 sites (six at 2.85 Å and additional six at 3.18 Å) of which only six can simultaneously be occupied. The additional distances of 2.2 Å between Na2 and adjacent O2 and O3 appear to be rather short but these oxygen sites would complete eight-fold coordination. Na3 has eight-fold coordination with O1 forming a six-membered ring around Na3 (Na3–O1: 2.68 Å) and two O2, one above and one below the six-membered ring (Na3–O2: 2.61 Å). There are actually three O2 sites each above and below the ring but the O2–O2 distances are too short to allow simultaneous occupation of all three sites.

TABLE 2b
Atomic Coordinates, Populations, and Displacement Parameters ($\times 10^2$) for Quenched $Na_{1.70}Ln_{0.10}\square_{0.20}SO_4$ (Ln = La, Yb)

Atom	Pop.	x	y	z	$U_{11}{}^a$	U_{22}	U_{33}	U_{23}	U_{13}	U_{12}
S1	0.44(4)	1/3	2/3	1/4	2.4(1)					
S2	0.28(2)	1/3	2/3	0.201(3)	4.0(2)					
Na1	0.898(4)	0	0	0	7.0(1)	U_{11}	4.1(1)	0	0	$1/2U_{11}$
Ln1	0.102(4)	0	0	0	7.0(1)	U_{11}	4.1(1)	0	0	$1/2U_{11}$
Na2	0.19(2)	1/3	2/3	0.677(4)	3.2(4)					
Na3	0.47(5)	1/3	2/3	3/4	3.9(4)					
O1	0.80	0.1831(5)	2x	1/4	7.8(3)	3.1(2)	11.3(7)	0	0	$1/2U_{22}$
O2	0.18	0.235(2)	2x	0.093(3)	13.3(13)	4.5(9)	7.5(11)	−3.2(11)	$1/2U_{23}$	$1/2U_{22}$
O3	0.28	1/3	2/3	0.014(7)	15.8(20)					

$^a U_{11}$ or U_{iso}.

TABLE 3
Bonding Distances (Å) and Selected Interatomic Angles (°)
for Slowly Cooled Na$_{1.70}$Ln$_{0.10}$□$_{0.20}$SO$_4$ (Ln = La, Yb)

S1–O1	2×	1.402(3)	S2–O3	1×	1.39(3)
S1–O2	2×	1.45(1)	S2–O1	3×	1.463(4)
O1–S1–O1	2×	107.6(3)	O1–S2–O1	3×	112.1(3)
O1–S1–O2	2×	107.6(2)	O3–S2–O1	3×	106.7(3)
O2–S1–O2	2×	105(1)			
Na1–O1^a	6×	2.468(2)	Ln1–O1	6×	2.468(2)
Na1–O2^a	6×	2.31(1)	Ln1–O3	6×	3.087(1)
Na2–O1^a	6×	2.713(4)	Na3–O1	6×	2.677(2)
Na2–O2^a	6×	2.85(1)	Na3–O2	2×	2.61(1)
Na2–O2	1×	2.20(2)			
Na2–O3	1×	2.23(4)			

^{a} Either O1 or O2 may be occupied; thus the coordination of Na1 is six-fold and the one of Na2 is eight-fold.

In none of the previous studies on Na$_2$SO$_4$ phase I structures have the S2 and O3 positions been located although Eysel *et al.* (17) discuss the possibility of this type of SO$_4$ disorder. It is striking that Na1 may form six additional bonds to O3 of 3.09 Å and that the numerical values of (La,Yb) on Na1 (contributing 0.06 La pfu) and O3 (0.38 O pfu) almost perfectly match this 1/6 ratio. This may suggest that the driving force for the position of O3 is actually Ln^{3+} on Na1. The three-valent charge of Ln^{3+} requires additional bonding partners to compensate for the higher valence compared to Na (Fig. 3). Thus, Ln^{3+} attracts oxygen toward O3 and the SO$_4$ tetrahedron is dragged to a position and orientation observed as S2 (Fig. 2). The position of O3 may also cause the disorder between closely spaced Na2 and Na3. Let us assume that the distance of 1.79 Å between Na3 and O3 (both atoms are positioned on the same three-fold axis) is too short, then O3 must be either neighbored by vacancies on Na3 or Na moves to Na2 which
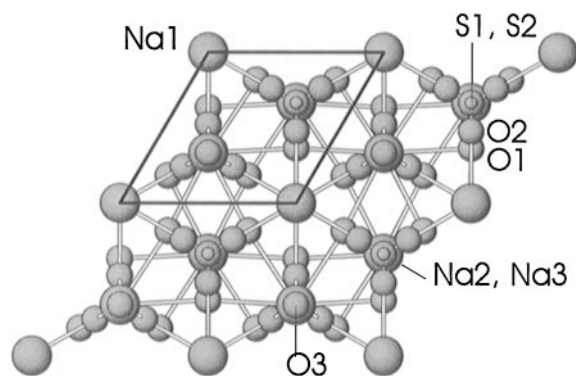

FIG. 2. Disorder of SO$_4$ tetrahedra in (La,Yb)-doped Na$_2$SO$_4$ phase I. (A) Observed distribution of disordered SO$_4$ tetrahedra; note the disorder is produced by a horizontal and a vertical mirror plane and by a vertical three-fold axis (parallel to *c*). Two types of S sites (characterized by small displacement ellipsoids) are distinguished, S1 (62% occupied) and S2 (19% occupied). S1 is at the intersection of the horizontal mirror plane with the three-fold axis; S2 is also on the threefold axis but displaced from the horizontal mirror plane and thus repeated. There are three symmetry independent but partially occupied O sites. O1 (78% occupied) is on the horizontal mirror plane, O2 (21% occupied) is on the vertical mirror plane, and O3 (19% occupied) is on the three-fold axis. (B and C) Tetrahedral coordination of S2 by one O3 and three O1. (D, E, F) Tetrahedral coordination of S1 by two O1 and two O2.

exhibits a Na2–O3 distance of 2.23 Å (Fig. 4). The fact that we have only 0.12 vacancies pfu but 0.38 O3 pfu indicates that O3 must have few short Na2–O3 distances. The number of these short Na2–O3 distances may be the limiting factor for the stability of this structure type with more extensive Ln^{3+} substitution.

FIG. 1. Structure of Ln^{3+}-doped Na$_2$SO$_4$ phase I projected parallel to *c* with unit cell outlines. Large spheres denote Na and Ln^{3+}, medium sized spheres are O, small spheres are S. Bonds are drawn between Na and O. Notice that all O sites are only partially occupied.
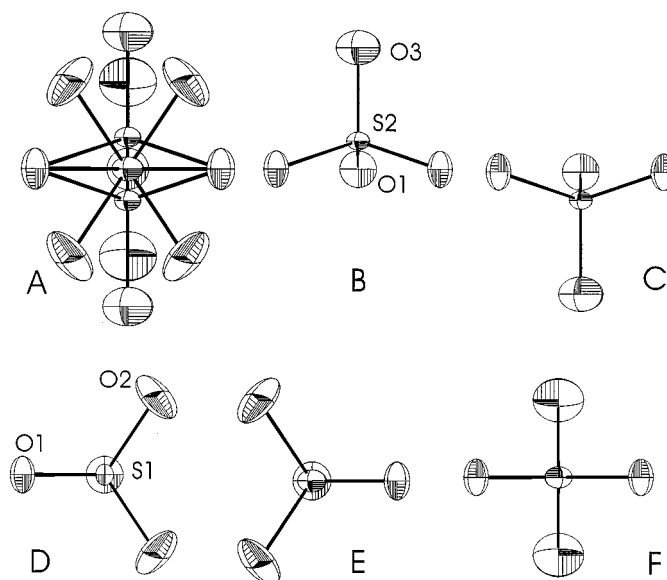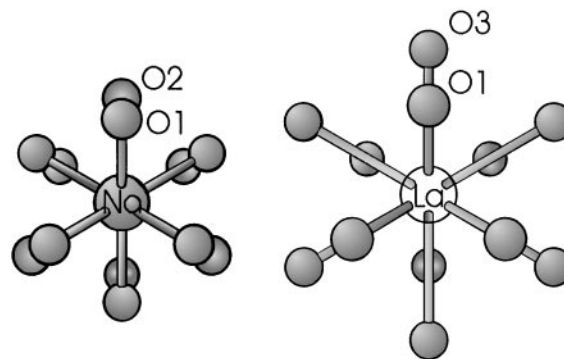

FIG. 3. Coordination of Na and La on Na1. Na exhibits a distorted octahedral coordination where O1 (Na–O1: 2.47 Å) and O2 (Na–O2: 2.31 Å) are statistically occupied. La has a regular octahedral coordination by O1 (La–O1: 2.47 Å) with additional six O3 atoms 3.09 Å apart.
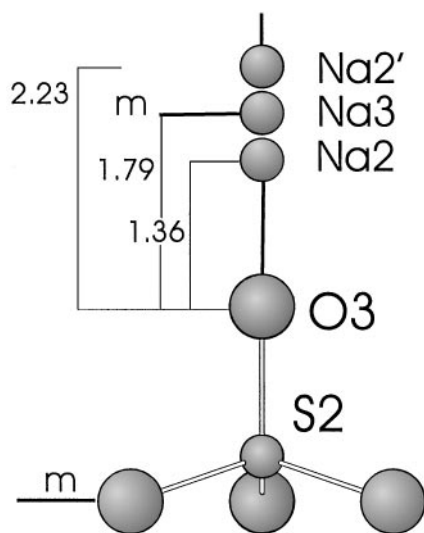
FIG. 4. Local neighborhood of S2 type SO_4 tetrahedra (*c*-axis vertical); *m* indicates horizontal mirror planes; two digit numbers represent distances in Å from O3 to adjacent Na sites. S2 type tetrahedra are only occupied if Na on Na1 is replaced by *Ln*. O3 forming the apex of the tetrahedron is only 1.79 Å apart from Na3 positioned on a mirror plane; thus Na3 must be vacant if O3 is occupied. O3 may either be bonded to Na2′ or Na2 and Na2′ may be vacant.

STRUCTURAL DIFFERENCES OF THE QUENCHED CRYSTALS

All three quenched structures (Y-, Yb-, and (La,Y)-substituted) and the slowly cooled (La,Yb)-substituted crystal have within 5 σ the same coordinates. The same good agreement is observed for the displacement parameters among the three quenched structures. However, the slowly cooled (La,Yb)-substituted crystal has displacement parameters for the positions S2, O3, and Na1 decreased by a factor of ca. 0.5–0.6 relative to the quenched structures. The displacement parameter of O1 is decreased by a factor of ca. 0.7 in the slowly cooled crystal. The remaining displacement parameters agree again within 5 σ. In other words, the entire S2 tetrahedron is better defined in the slowly cooled sample but displays substantial disorder in the quenched structures. One has to consider that O1 is shared by S1 and S2 which explains the moderate decrease of the O1 displacement parameter in the slowly cooled crystal. As discussed above, the correlation between substituting Me^{3+} on Na1 and the presence of the S2 tetrahedron is also reflected in the common behavior of displacement parameters of these entities.

The major differences between the quenched and the slowly cooled (La,Yb)-substituted structure are the atomic populations (Table 2). The much higher population of Ln^{3+} on Na1 in the quenched sample causes also an increase of the population of the S2 tetrahedron relative to the slowly cooled crystal (Tables 1 and 2). As already found for the

slowly cooled crystal the number of S2 tetrahedra per formula unit and Ln^{3+} pfu on Na1 is related by a factor of 6/1.

At first glance one could speculate that slow cooling causes exsolution of a more Ln^{3+} rich phase which, due to its low concentration, is not picked up by the diffraction experiments. Furthermore, one could assume that the weak diffuse "superstructure" reflections are actually diffraction spots of this additional exsolved phase. There are, however, convincing arguments contradicting this assumption. Eysel *et al.* (17) showed that increasing substitution of Y^{3+} or Ni^{2+} in Na_2SO_4 phase I causes a significant increase of the *a*-axis and a strong decrease of the *c*-axis, whereas the cell volume remained almost constant. This behavior of cell dimensions is not observed (Table 1) for the quenched phase with assumed high Ln^{3+} concentration and the slowly cooled phase with assumed low Ln^{3+}. Furthermore, the cell volume of the quenched crystal (176.9 Å^3) increases to 178.5 Å^3 when slowly cooled. In addition, the exsolution model cannot explain the stronger disorder of S2 tetrahedra in the quenched samples as evidenced by the increased displacement parameters. For the above reasons we assume that the two crystals with different cooling histories have the same chemical composition. Thus the lower Ln^{3+} content located in the structure of the slowly cooled sample is probably an artifact caused by correlation effects between the scale factor and atomic populations.

It is well known that cation ordering leads to an increase of the cell volume as found for the slowly cooled crystal (other examples for this behavior are the tetrahedral framework structures of cordierite (27) and feldspars (28) with ordered and disordered Si, Al distributions). An ordering model for the slowly cooled crystal would also be in agreement with the better defined S2 tetrahedra, the presence of superstructure reflections, and the well established high ionic conductive for this structure type (20).

Similar superstructure reflections, leading to a tripling of the *c*-axis, have also been reported (29) for burkeite, $Na_4SO_4(CO_3)_t(SO_4)_{1-t}$. This mineral has a structure closely related to Na_2SO_4 with CO_3 units partially replacing SO_4 tetrahedra. The burkeite structure is orthorhombic (*Pmnm*) with cell dimension of ca. $a = 5.17$, $b = 9.21$, $c = 7.06$ Å. If the *b* dimension is divided by 3 a pseudo-hexagonal setting corresponding to Na_2SO_4 phase I is obtained. The superstructure reflections in burkeite (29) were attributed to ordering of SO_4 orientations (disordered in the subcell). Similar arguments may hold for the superstructure reflections in slowly cooled Ln^{3+}-substituted Na_2SO_4. If we further assume that mainly the S1-type tetrahedra are involved in ordering in Ln^{3+}-substituted Na_2SO_4, it has to be considered that complete order cannot be achieved because of the additional S2-type tetrahedra with apical oxygen on the three-fold axis. In addition to ordering of SO_4 orientations, there seems also to be ordering of Ln^{3+} and vacancies on the sites Na1, Na2, and Na3 upon slow cooling. In the

refinement model for the slowly cooled sample we assume, in analogy to the quenched crystals, complete occupancy of Na1 by Na and (La, Yb). This might not be correct and instead vacancies may also occur on Na1 or some Ln^{3+} diffused to Na2 and Na3. However, the structure refinement only allows the determination of the number of electrons on a specific atomic site; thus, the exact model cannot be resolved. At first glance, the above discussion may be misleading if one assumes that in the quenched structure Ln^{3+} is concentrated on Na1 but becomes "disordered" on Na2 and Na3 in the slowly cooled crystal. One has to consider that the exact structure of the slowly cooled crystal (tripled c-axis) has not been determined and all discussions are based on the subcell. What looks like increased disorder in the subcell may well be increased ordering in the supercell.

COMPARISON WITH OTHER STRUCTURAL STUDIES ON Na$_2$SO$_4$ PHASE I

All structures refined in this study are closely related to the one of Na$_2$SO$_4$ phase I stable above 510 K (11, 14). So far, two quenched structures of Y (2.1%) and Nd (2.7%) doped Na$_2$SO$_4$ were reported at ambient conditions (17, 22). Compared to our results these previous studies show significant differences. These difference may be either realistic or the true defect structure in the previous studies could not completely be resolved due to insufficiencies of the data or the refinement model.

All phase I varieties have the following structural features in common: Within $P6_3/mmc$ space group symmetry Na ions (type Na2 and Na3) and SO$_4$ tetrahedra are alternately "spit" along the three-fold axes at 1/3, 2/3, z and 2/3, 1/3, z. Additional Na (type Na1), hosted at the origin and 0, 0, 1/2, has $\bar{3}m$ symmetry. The bonding requirements of Na1 are mainly responsible for the variability of phase I. It must be stressed, however, that within space group $P6_3/mmc$ an ordered tetrahedral arrangement cannot be assembled. The Na1–O bonds vary with temperature and partial substitution by different charged cations. Various Na1–O distances can be accomplished by rotation or small shifts of the rigid SO$_4$ tetrahedra.

Rasmussen et al. (11) used powder X-ray Rietveld data collected at 543 K refined with the starting parameters of Eysel et al. (17) and determined two oxygen sites. One site (O1) with local symmetry $m..$ (multiplicity 12) is 1/3 occupied and the other (O2) with $.m.$ symmetry (at x, y, 1/4, multiplicity 12) is also 1/3 occupied. This model leads to S–O2 of 1.35 Å and S–O1 of 1.43 Å. Na1–O distances are between 2.47 and 2.50 Å and those of Na2 are between 2.44 and 2.60 Å. It remains actually dubious whether the refined oxygen distribution is correct or a consequence of the applied model which was adopted from an Y-substituted structure (17). The O2 site is very close (0.25 Å) to a position

of $mm2$ symmetry (at ca. 0.19, $2x$, 1/4) which is essentially identical to our O1 site.

Naruse et al. (14) reported single-crystal X-ray data at 693 K and described a slightly different oxygen arrangement. In their structure both O sites have $m..$ symmetry leading to S–O2 of 1.33 Å and S–O1 of 1.58 Å. Their O2 is at 0.193, $2x$, 0.226 similar to our O1 site but slightly displaced parallel to the three-fold axis. Oxygen populations are not given but from the specified tetrahedral S coordination (3 × O2 and 1 × O1) one has to assume that O1 is 1/6 occupied and O2 is 1/2 occupied. Na1–O distances are between 2.46 and 2.71 Å and Na2–O distances are between 2.28 and 2.74 Å. The authors emphasize that the disorder may be more extensive but could not be evaluated in detail in order to keep the ratio between parameters and observations at a reasonable value.

Eysel et al. (17) studied the quenched structure of Na$_{1.88}$Y$_{0.04}$□$_{0.08}$SO$_4$ at room temperature and developed a model structure for end-member Na$_2$SO$_4$. We may suspect that due to the relatively low Y substitution, additional O and S disorder could not be determined. Furthermore, cation vacancies were not resolved in this study and the oxygen coordinates were modeled from the structure refinement and crystal chemical principles. Our study on quenched Na$_{1.82}$Y$_{0.06}$□$_{0.12}$SO$_4$ shows Y concentrated together with Na on Na1. There are vacancies on Na2 and Na3, and 0.34 SO$_4$ pfu are of the S2 type with the remainder being of S1 type.

A room-temperature structure of Na$_{1.85}$Nd$_{0.05}$□$_{0.10}$SO$_4$ was reported by Rastsvetaeva and Andrianov (22). The authors also note additional diffuse reflections but did not characterize them. It remains unclear whether the crystal was slowly cooled or quenched but the presence of additional reflections may indicate slow cooling. In agreement with our study, an additional O3 site was found completing the Nd coordination. However, in contrast to our investigation only one S site was found and O3 is displaced from the three-fold axis and has a much higher population than expected from the low Nd substitution. This model led to S–O distances between 1.39 and 1.56 Å with corresponding O–S–O angles between 94 and 120°. For local Nd^{3+} on Na1 nine-fold coordination by 6 × O2 of 3.18 Å and 3 × O3 of 2.38 Å was assumed whereas for Na on Na1 octahedral coordination by either 3 × O1 of 2.45 Å and 3 × O2 of 2.18 Å or 6 × O1 of 2.45 Å was predicted.

CONCLUSION

In the present room temperature structural study on quenched Na$_{1.76}$Yb$_{0.08}$□$_{0.16}$ SO$_4$, Na$_{1.82}$Y$_{0.06}$□$_{0.12}$SO$_4$, quenched and slowly cooled Na$_{1.70}$Ln$_{0.10}$□$_{0.20}$SO$_4$, (Ln^{3+} = La, Yb) an additional O site (O3) could be found which locally completes the Ln^{3+} coordination and is responsible for the arrangement of SO$_4$ units according

to S2 in Fig. 2. Furthermore, additional few faint and diffuse reflections were observed for slowly cooled $Na_{1.70}Ln_{0.10}\square_{0.20}SO_4$, $(Ln^{3+} = $ La, Yb) leading to tripling of the c-axis. This tripling is not consistent with any of the known low temperature structures of Na_2SO_4 (11). We suspect that additional long-range ordering is present in the investigated crystal, but this order could not be resolved due to the faint character of the additional reflections which made the determination of the space group for the "true" structure impossible.

The various structures refined for phase I of Na_2SO_4 allow some general rules for the stability of this phase to be derived. For *pure* Na_2SO_4 displacive phase transitions to phase II (space group *Pbnm*) and phase III (space group *Cmcm*) prohibit quenching of phase I (space group $P6_3/mmc$) down to room temperature. Phase II and III have long-range ordered SO_4 arrangements where the general distribution of S and Na sites remains the same as in phase I. Such an ordered arrangement of SO_4 units can be disturbed by incorporation of high valent cations associated with vacancies replacing Na. The different charge and size of the substituting ion leads to additional orientations of SO_4 entities (S2-type) that stabilizes the disordered high-temperature structure of phase I which under these conditions can be quenched to room temperature. In other words, upon cooling the substituting ions do not allow spontaneous formations of structures with ordered SO_4 arrangements as described for phases II and III. This behavior finally allows the growth of large single crystals necessary for possible laser applications of this new host material.

REFERENCES

1. S. A. Payne, W. F. Krupke, L. K. Smith, L. D. DeLoach, and W. L. Kway, *OSA Proc. Adv. Sol. State Lasers* **13,** 227 (1992).
2. C. D. Marshall, L. K. Smith, R. J. Beach, M. A. Emanuel, J. A. Skidmore, H. T. Powell, and W. F. Krupke, *OSA Proc. Adv. Solid State Lasers* **24,** 333 (1995).
3. D. S. Sumida, T. Y. Fan, and R. Hutcheson, *OSA Proc. Adv. Solid State Lasers* **24,** 348 (1995).
4. E. Mix, G. Huber, D. Ehrt, W. Seeber, *OSA Proc. Adv. Solid State Lasers* **24,** 339 (1995).
5. D. C. Hanna, J. K. Jones, A. C. Large, D. P. Shepherd, A. C. Tropper, P. J. Chandler, M. J. Rodman, P. D. Townsend, and L. Zhang, *Optics Comm.* **99,** 211 (1993).
6. N. V. Kuleshov, A. A. Lagatsky, A. V. Podlipensky, and V. P. Mikhailov, *Opt. Lett.* **22,** 1317 (1997).
7. D. S. Sumida, *OSA Proc. Adv. Solid State Lasers* **24,** 348 (1995).
8. L. D. DeLoach *et al.*, *J. Opt. Soc. Am. B* **11,** 269 (1994).
9. K. I. Schaffers, L. D. DeLoach, and S. A. Payne, *IEEE J. Quant. Electr.* **32,** 741 (1996).
10. G. Dahrmasena and R. Frech, *J. Chem. Phys.* **99,** 8929 (1993).
11. S. E. Rasmussen, J.-E. Jørgensen, and B. Lundtoft, *J. Appl. Cryst.* **29,** 42 (1996).
12. B. N. Mehrotra, Th. Hahn, H. Arnold, and W. Eysel, *Acta Cryst. A* **31,** S79 (1995).
13. R. McL. Murray and E. A. Secco, *Can. J. Chem.* **56,** 2616 (1978).
14. H. Naruse, K. Tanaka, H. Morikawa, and F. Marumo, *Acta Cryst. B* **43,** 143 (1987).
15. H. F. Fischmeister, *Mh. Chem.* **93,** 420 (1962).
16. K. L. Keester, W. Eysel, and Th. Hahn, *Acta Cryst. A* **31,** S79 (1985).
17. W. Eysel, H. H. Höfer, K. L. Keester, and Th. Hahn, *Acta Cryst. A* **41,** 5 (1985).
18. M. A. Bredig, *J. Phys. Chem.* **47,** 587 (1943).
19. M. Vlasse, C. Parent, R. Salmon, G. Le Flem, and P. Hagenmuller, *J. Solid State Chem.* **35,** 318 (1980).
20. P. P. Fedorov, T. M. Polkhovskaya, B. P. Sobolev, A. K. Ivanov-Shits, and N. I. Sorokin, *Sov. Phys. Cryst.* **28,** 353 (1983).
21. H. H. Höfer and W. Eysel, *J. Solid State Chem.* **36,** 365 (1981).
22. R. K. Rastsvetaeva and V. I. Andrianov, *Sov. Phys. Dokl.* **30,** 341 (1985).
23. P. Mikhail, R. Basler, and J. Hulliger, submitted.
24. "Structure determination package (SDP)." Enraf Nonius, Delft, The Netherlands, 1983.
25. G. M. Sheldrick, "SHELX97, Program for crystal structure determination." University of Göttingen, Germany, 1997.
26. R. D. Shannon, *Acta Cryst. A* **32,** 751 (1976).
27. Th. Armbruster and F. D. Bloss, *Contrib. Miner. Petrol.* **78,** 732 (1981).
28. H. Kroll and P. H. Ribbe, *Rev. Miner.* **2,** 57 (1983).
29. G. Giuseppetti, F. Mazzi, and C. Tadini, *N. Jb. Miner. Mh.* **1988,** 203 (1988).